Biosensors and Bioelectronics 40 (2013) 174–179

Contents lists available at SciVerse ScienceDirect

Biosensors and Bioelectronics

journal homepage: www.elsevier.com/locate/bios

Impedance sensing and molecular modeling of an olfactory biosensor based on chemosensory proteins of honeybee

Qingjun Liu [a], Hua Wang [a], Hongliang Li [b], Jing Zhang [c], Shulin Zhuang [c], Fenni Zhang [a], K. Jimmy Hsia [d], Ping Wang [a,*]

[a] Biosensor National Special Laboratory, Key Laboratory of Biomedical Engineering of Education Ministry, Department of Biomedical Engineering, Zhejiang University, Hangzhou 310027, PR China
[b] College of Life Sciences, China Jiliang University, Hangzhou 310018, PR China
[c] College of Environmental and Resource Sciences, Zhejiang University, Hangzhou,310058, PR China
[d] Department of Mechanical Science and Engineering, University of Illinois at Urbana-Champaign, Urbana, IL 61801, USA

ARTICLE INFO

Available online 21 July 2012

Keywords:
Chemosensory protein
Olfactory biosensor
Impedance
Molecular modeling
Honeybee

ABSTRACT

By mimicking biological olfaction, biosensors have been used for the detection of important ligands in complex environments. An olfactory biosensor based on chemosensory proteins (CSPs) was designed by immobilizing honeybee CSPs (Ac-ASP3) on the interdigitated golden electrodes. Its responses to ligands of pheromones and floral odors were recorded by impedance spectroscopy. The relative decrease of charge transfer resistance of the biosensor is proportional to the logarithm of ligand concentration from 10^{-7} M to 10^{-3} M. To explore the molecular recognition processes of the biosensor, the tertiary structure of the protein was modeled and the protein-ligand interactions were investigated by the molecular docking. Our docking results verified the validity of experiments and showed that the specific ligands could form hydrogen bonds with some of the conserved residues, such as Cys 60 and Gln 64 of Ac-ASP3. Furthermore, combining the molecular modeling with impedance detection, the accuracy, specificity and predictability of the ligands binding to the protein could be improved. Thus, CSPs will provide a promising approach for chemical molecular sensing at low concentrations.

1. Introduction

The olfactory system has the ability to discriminate and identify thousands of odorant compounds at very low concentration. The discovery of membrane-bound olfactory receptors (ORs), in both vertebrates and insects, has shown that they can be directly activated by messenger molecules of odorants and pheromone molecules (Buck and Axel, 1991). At the same time, the soluble proteins in high concentration around ORs, which indicate lots of important chemosensory roles, particularly in insects, are mainly classified as odorant-binding proteins (OBPs) and chemosensory proteins (CSPs) (Pelosi et al., 2005; Vieira and Rozas, 2011). Insects can recognize a wide range of chemical signals across animal species and between congener, during which these sensory proteins play a critical role. The chemosensation guide perception of the surrounding environment, detection of predators and location of food and hosts for insects.

The understanding of the biological olfactory system provides valuable insight into odor detection, especially by biosensors. In recent years, many researchers have been trying to develop olfactory biosensors based on olfactory system (Vidic, 2010; Lee and Park, 2010; Glatz and Bailey-Hill, 2011). In those olfactory biosensors studies, ORs have been the very commonly used sensing elements. In the biosensor system, ORs could be activated by odorant molecules, and then the biology interactions are translated into electrical signals just as what happens to the central nervous system (Minic et al., 2005; Lee and Park, 2010; Liu et al., 2010). However, ORs are G protein coupled receptors, which need to stay in their cellular membrane environment to be functional, so that there are inherent difficulties associated with the availability of ORs. OBPs could increase the solubility of volatile hydrophobic odors and make them available to the ligand-binding site of ORs. So OBPs also act as potential sensing materials in olfactory sensors (Ko and Park, 2008; Hou et al., 2005; Sankaran et al., 2010). CSPs represent another protein family that could bind and transport pheromones or other ligands, associated with conformational changes, but they are barely used in olfactory biosensors.

Insect CSPs, which had been identified in several chemosensory as well as non-chemosensory tissues, are deduced to be multifunctional context-dependent proteins involved in diverse cellular processes (Picimbon et al., 2000; Pelosi et al., 2005).

* Corresponding author. Tel.: +86 571 87952832; fax: +86 571 87951676.
E-mail address: cnpwang@zju.edu.cn (P. Wang).

0956-5663/$ - see front matter © 2012 Elsevier B.V. All rights reserved.
http://dx.doi.org/10.1016/j.bios.2012.07.011

Besides mediating the solubilization of hydrophobic odorants, CSPs can bind different lipophilic ligands, so that they are believed to be involved in chemical communications, including perception, identification, transport and transduction of semiochemicals from environments (Briand et al., 2002; Ozaki et al., 2008). Moreover, CSPs are stable in a wide range of pH and temperature, which offers an access to large quantity of CSPs expressed in prokaryote for further research (Picone et al., 2001). All of these facts suggest that CSPs possibly provide a new recognizing approach for olfactory biosensor.

Honeybees, which are able to discriminate among a wide range of odors, have been trained to detect specific odors related to explosives, mines and drugs (Repasky et al., 2006; Rains and Tomberlin, 2008). The honey bee CSPs represent the multifunctional insect CSPs family and become attractive models for gaining insights into the organization and function of the olfactory system, as well as the underlying mechanisms of associative olfactory learning (Forêt et al., 2007; Li et al., 2007). This paper focuses on a kind of antennal CSP of Chinese honeybee, *Apis cerana cerana* (Ac-ASP3), with a purpose of detecting its binding properties. Impedance based biosensors are particularly suited for the detection of binding events on the transducer. An impedance biosensor was designed to detect the binding reactions between Ac-ASP3 and the ligands of pheromones and floral odors. On the other hand, to illuminate the ligand binding and explore the essence of biological reaction, the molecular recognition process was simulated by means of molecular docking. And the correlations between protein conformation and electrical impedance properties were discussed.

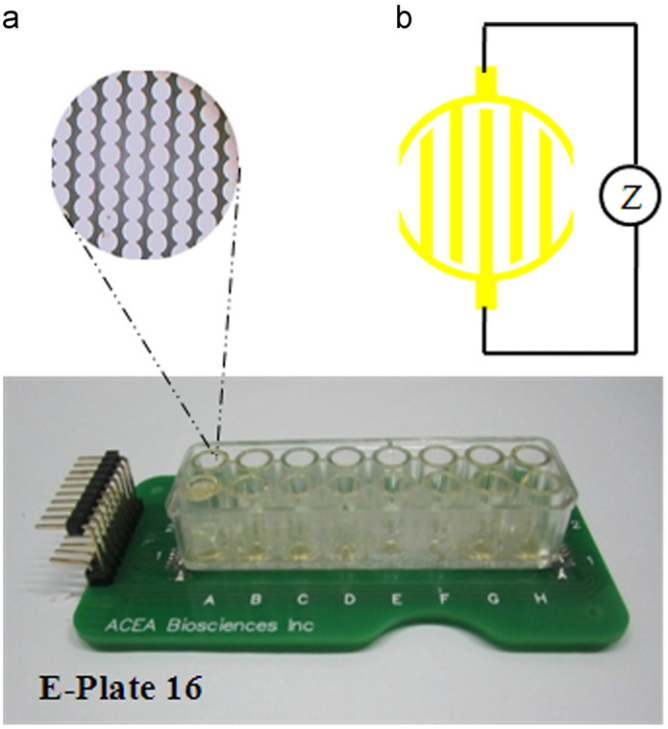

Fig. 1. E-Plate 16 device of the biosensor system. (a) Circle-on-line interdigitated electrodes on the bottom of a well; (b) Sketch map of the impedance measurement of the electrodes.

2. Experiment

2.1. Protein and ligands

The biologically active recombinant Ac-ASP3, whose molecular weight is 18 kD, was cloned from the full-length cDNA of adult worker bees in Chinese honeybee, *Apis cerana cerana* (Li et al., 2007). The protein was prepared in phosphate buffer solution (PBS, pH = 7.4) with a concentration of 130.67 μg/mL.

Ligands of CSPs mostly focus on general volatile odors and pheromones. In this paper, worker bee pheromone (geraniol) and alarm pheromone (isoamyl acetate), with a kind of floral odor (phenyl acetaldehyde) were chosen as tested ligands, additionally, 4-allylveratrole, 3,4-dismethylbenzaldehyde, β-ionone and methy-*p*-hydroxyl benzoate were tested as well. The ligands from 10^{-7} M to 10^{-4} M were diluted with PBS from original concentration of 1 mM in methanol. These reagents were all purchased from Sigma-Aldrich (USA).

2.2. Electrodes processing and electrochemical measurement

The electronic plate (E-Plate 16) with interdigitated electrodes in the bottom of the 16 wells was obtained from ACEA Biosciences Inc. (USA) (shown in Fig. 1). The interdigitated electrodes are circle-on-line electrodes. The diameter of the circle is 90 nm. The width of the line is 30 nm. The distance between two adjacent pairs of electrodes is 80 nm. The electrodes cover approximately 80% of the bottom areas of each well, which allows for maximal sensitivity for the detection of the electrochemical reactions at the electrode interface, with relatively uniform distribution of the electric field while maximizing the coverage area of each well. It has been used successfully for dynamic monitoring of live cells by real-time impedance detection (e.g., Abassi et al., 2004; Atienza et al., 2006). Before protein immobilization, the interdigitated electrodes were cleaned with ultrapure water and dried under nitrogen flow. Nitrocellulose membrane has been used for immobilization of proteins, with its microporous nature of large volume to surface area ratio and high binding capacity to biomolecules, which provides a tremendous number of binding sites per unit area. Several lines of evidence indicate that biomolecules interact with nitrocellulose via a non-covalent, hydrophobic interaction. The nitrocellulose membrane was obtained from Shanghai Haoran Biological Technology Co. (China). Firstly, nitrocellulose dissolved in methanol was added into plate wells in a 5 μL volume which could coat electrodes completely. After about 10 min until the methanol evaporated off, a membrane of nitrocellulose was left on the electrodes. At last, Ac-ASP3 solution was injected into plate wells. A 2-h waiting period was needed to guarantee that the protein molecules were embedded in the nitrocellulose membrane. The residual solution was then drained out with PBS. These operation steps were all conducted at room temperature (18–25 °C).

Electrochemical measurements were performed using the Zahner ZENNIUM electrochemical workstation with the THALES software (Zahner Elektrik, Germany). One pole of the interdigitated electrodes was connected to both the test and sense probes on the electrochemical workstation, and another pole was connected to both the reference and counter probes on the electrochemical workstation (Fig. 1).

The tested frequency was set in the range from 1 Hz to 100 kHz with a 5 mV AC voltage in the impedance measurement program. Ligands at different concentrations were added to the plate wells containing 5 mM K4[Fe(CN)6]/K3[Fe(CN)6] (1:1). At each concentration, electrochemical impedance spectroscopy was recorded for about 40 min. After each measurement, the well was rinsed by PBS for about 15 min. All of electrochemical measurements were performed at room temperature (18–25 °C).

2.3. Molecular modeling

The tertiary structure of Ac-ASP3 was built by I-TASSER server (Zhang, 2008). Based on the amino acid sequence of Ac-ASP3

(Li et al., 2007), the server first tried to retrieve initial template from the PDB library by LOMETS, a locally installed meta-threading approach. Then the continuous fragments excised from the PDB templates were reassembled into full-length models. After the model selection, refinement and structure-based functional annotation, the quality of the obtained model was further evaluated by the Prosa web server.

To predict the binding modes of different ligands to Ac-ASP3, the ligands were docked into the binding site of Ac-ASP3 using the Molegro Virtual Docker (MVD) Version 4.2 following default protocols. The binding pocket covers a site with a user-defined origin and a radius of 15 Å. MolDock SE was used as the searching algorithm. The energetic evaluations of the complexes were implemented with MolDock Score. For each molecular docking, 10 poses were finally obtained and the best pose with the highest docking score was selected for the analysis.

Thereafter, with a theoretical model, we discussed the correlations between the conformational changes of the protein and impedance spectrum changes of the biosensor.

3. Results and discussion

3.1. Impedance sensing

In the presence of redox probe, electrochemical cell could be modeled to the Randles cell, shown in the inset of Fig. 2. The circuit includes four elements: the ohmic resistance of electrolyte solution, Rs; the constant phase element, CPE; the Warburg impedance, Zw; and the charge transfer resistance, Rct (Lisdat and Schäfer, 2008). The parallel elements are introduced because the total currents (i) through the working electrode is the sum of distinct contributions from the Faradic process (i_f) and double layer charging (i_c). Since all the currents must pass through the uncompensated solution resistance, Rs is inserted as a series element in the equivalent circuit (Katz and Willner, 2003). Rs and Zw represent bulk properties of the electrolyte solution and diffusion of the redox probe, respectively. CPE and Rct both depend on the dielectric and insulating features at the electrode/electrolyte interface, and they are affected by the property change occurring at the interface. After the electrochemical measurement, we simulated the Nyquist plots (Zre VS. -Zim) recorded in the experiment by Zview (Scribner Associates Inc., US). Through comparison, among these four parameters, the change of Rct is the most obvious, so that Rct is chosen as the sensing parameter. The diameter of the semicircle part of the Nyquist plot is equal to Rct.

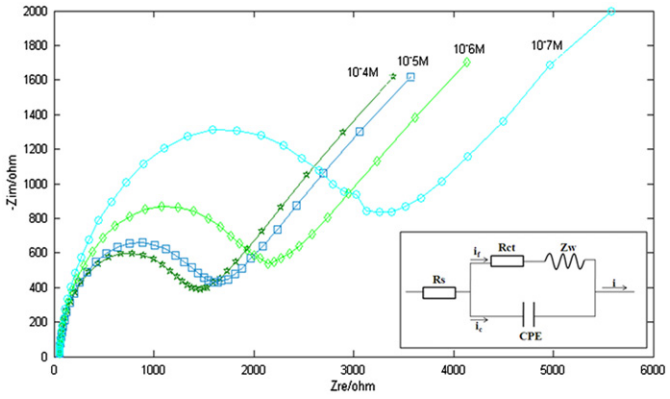

Fig. 2. Nyquist plots of impedance spectra at various isoamyl acetate concentrations from 10^{-7} M to 10^{-4} M. The symbols are the experimental data and the lines represent the stimulated spectra. Randles cell is shown in the inset.

After the immobilization of Ac-ASP3, the area of the electrodes decreased apparently and the attachment of protein would retard the interfacial electron-transfer kinetic and increase Rct significantly. After the injection of ligands, the binding reaction reached a steady state within 40 min (shown in Fig A.1 in Appendix). So, the data at 40 min, can be used as the representative data of the finally stabilized parameters. And, with increasing concentration, Rs and Zw kept constant, while CPE just changed slightly and Rct decreased significantly. Therefore, Rct is the appropriate parameter for sensing the protein-ligand interactions. Fig. 2 displays impedance spectra of isoamyl acetate as a typical Rct recording example.

This decrease of Rct should indicate the difference in the dielectric or conductive properties of the multilayer of nitrocellulose and proteins on the electrode, more narrowly, a more facile electron transfer at the electrode interface. After the injection of ligands, the mobile ions around the protein increased and the fixed charges together with the dipole-ion on the protein shifted from their initial position. All of them excluded local buffer ions, resulting in the changes of protein conformation, then the changes of the impedance.

After detailed analysis, we can see that the relative variation of Rct is linear for the logarithm of ligand concentration. The normalized impedance change (NIC) is described as NIC$=(Z_b-Z_a)/Z_b$, where Z_b represents Rct before the injection of ligand and Z_a represents Rct after the injection. Fig. 3 shows NIC of Ac-ASP3 as a function of different ligand concentration. On the whole, at low concentration, the impedance response resulting from physical absorptions is staple, and that resulting from specific binding is faint, therefore the change of Zw is significant but the change of Rct is weak. However, as the ligand concentration increases, specific binding is likely to be the dominant cause gradually, leading to more obvious change of Rct.

For bee alarm pheromone, isoamyl acetate, its regression equation is $y=0.048x+0.61$ ($R^2=0.966$) (Fig. 3a). The maximal variation of Rct can reach about 20%, from 10^{-7} M to 10^{-4} M. For worker bee pheromone, geraniol, its regression equation is $y=0.073x+0.62$ ($R^2=0.895$) (Fig. 3b). The maximal variation of

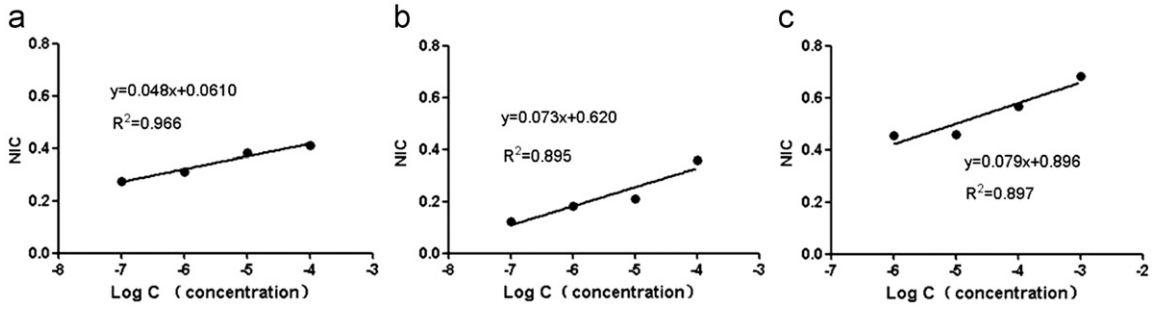

Fig. 3. The normalized impedance change (NIC) of Ac-ASP3 to different ligands. (a) isoamyl acetate; (b) geraniol; (c) phenyl acetaldehyde.

Rct comes to a head of about 30%, from 10^{-7} M to 10^{-4} M. For a floral odor, the regression equation of phenyl acetaldehyde is $y=0.079x+0.896$ ($R^2=0.897$) (Fig. 3c). Its maximal variation of Rct attains about 30% within the sensitive test range. The rest of tested ligands show poor specificity to Ac-ASP3 (shown in Fig A.2 in Appendix). According to the value of correlation coefficient R, the linearity of the three plots is pretty good. As we all known, pheromones are pretty specific for different insects. They can direct insect behavior. Honey bee pheromones can act as chemical signals to transmit information and regulate behavior. These special languages guarantee all kinds of unique reactions of the queen bee, worker bees and drones to the environment. As alarm pheromone, isoamyl acetate functions as a defensive substance to signal danger. While, besides being produced by many flowering plants, geraniol is also produced from honeybee glands as a pheromone. It can help mark nectar bearing flowers and find the entrance to their combs. In addition, floral odors acting as bee synomones can attract the bee to collect honey; on the other hand, they can favor plants pollination. According to the experimental results, we could infer that Ac-ASP3 is involved in pheromone molecules as well as floral odor perception.

Each ligand was tested for at least three times, and almost the same results were obtained from the distinct tests. Meanwhile, a blank test using the solvent was conducted. It is possible that solvent molecules can be absorbed or entrapped onto the multilayer of nitrocellulose and proteins by diffusion, resulting in some variation of the dielectric features at the electrode/electrolyte interface. Whereas the impact of solvent molecules was so weak that it could be ignored. Anyway, compared with the blank test, the impedance responses to specific ligands were very significant. The maximal variation of Rct could reach 20%–30% during the binding test, with a detection limit of 10^{-7} M for isoamyl acetate and geraniol, 10^{-6} M for acetaldehyde. The sensitivity should be enough for quantitatively detecting the ligands. Therefore, the biosensor has reserved the biofunction of Ac-ASP3 and it can be used to detect ligands selectively and quantitatively.

With Ac-ASP3's high sensitivity to bee pheromones and floral odors, this analytical tool can be introduced to beekeeping, performing searching and hunting dispersive bee colony. Furthermore, many olfactory ligands, important for insect biology, are similarly important in commercial application. Far and wide, the bio inspired biosensor offers potential applications for environmental monitoring, agriculture, anti-bioterrorism, disease diagnostics, and food safety.

3.2. Molecular modeling

Nowadays molecular modeling has been promoting the researches on biology and medicine. It has been used to investigate and analyze the configuration and physiological function of numerous concernful proteins. The combination of biosensor with molecular modeling can optimize the design of the sensor, and acquire useful information which could not be obtained through experiments. It helps improve accuracy, specificity and predictability of the ligands binding to the protein.

CSPs are well conserved with often > 50% of identical residues even between members of phylogenetically distant species. Fig. 4a is the tertiary structure of Ac-ASP3 shown in the wireframe mode. Their signature is constituted by four cysteines, which are connected by disulphide links between adjacent residues. Fig. 4b is the backbone structure of its six α-helices. These conserved conformations might constitute the ligand binding pocket. The α-helical domains determine the hydrophobicity of the protein, and then impact its binding property. Based on the modeled tertiary structure, we evaluated the binding interactions of Ac-ASP3 with different ligands by molecular docking. By analyzing the structure of the ligand- protein complex, the residues associated with binding interaction were identified.

Hydrogen bonds play an important role in the ligand-protein binding process. They are responsible for direction and recognition of substrates. They can also modify the affinity to their binding partners (Kubinyi, 2001; Nocker et al., 2009). In our study, we found different hydrogen bonds between different ligands and residues, shown with the blue dashed lines in Fig. 5. Cysteine, which has chelation, can link with poisonous isoamyl acetate. Oxygen atom of carbonyl group in isoamyl acetate is hydrogen bonded to Cys 60, shown in Fig. 5a. Isoamyl acetate lies parallel in the binding pocket. Their conformations match pretty well. Glutamine can easily react to alcohol and geraniol is a kind of monoterpene alcohol. Fig. 5b shows oxygen atom of alcohol in geraniol forms hydrogen bond with Gln 64. In the reaction, Gln 64 acts as hydrogen bond donor. The arginine side chain is a common hydrogen bond partner and it is often associated with carboxylic acid and phosphate groups of the ligand. Fig. 5c shows that the oxygen atom of carbonyl group in phenyl acetaldehyde forms hydrogen bond with Arg 97. It is obvious that Cys 60, Gln 64 and Arg 97 play an important role in the binding interactions.

From the amino acid sequence, we found that Cys 60 and Gln 64 are conserved amino acids of Ac-ASP3. As we all known, conserved amino acids of protein are the ones that keep changeless during insect evolution and play an important role in insect evolution. They are critical to the conformation and function of the protein. For example, conserved motifs exposed on the surface of the protein can be involved in protein regulation and interactions. It is obvious that the physiological function of Cys 60 and Gln 64 relates to the binding property of the protein. Of course, although Arg 96 is not conservative, its guanidine, which is active, may influence the binding property. These results indicate the

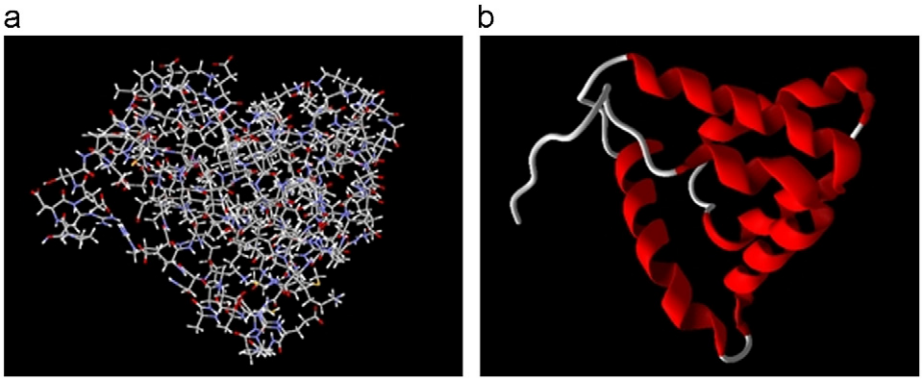

Fig. 4. Structure of Ac-ASP3 generated by homology modeling: (a) wireframe structure; (b) backbone structure.

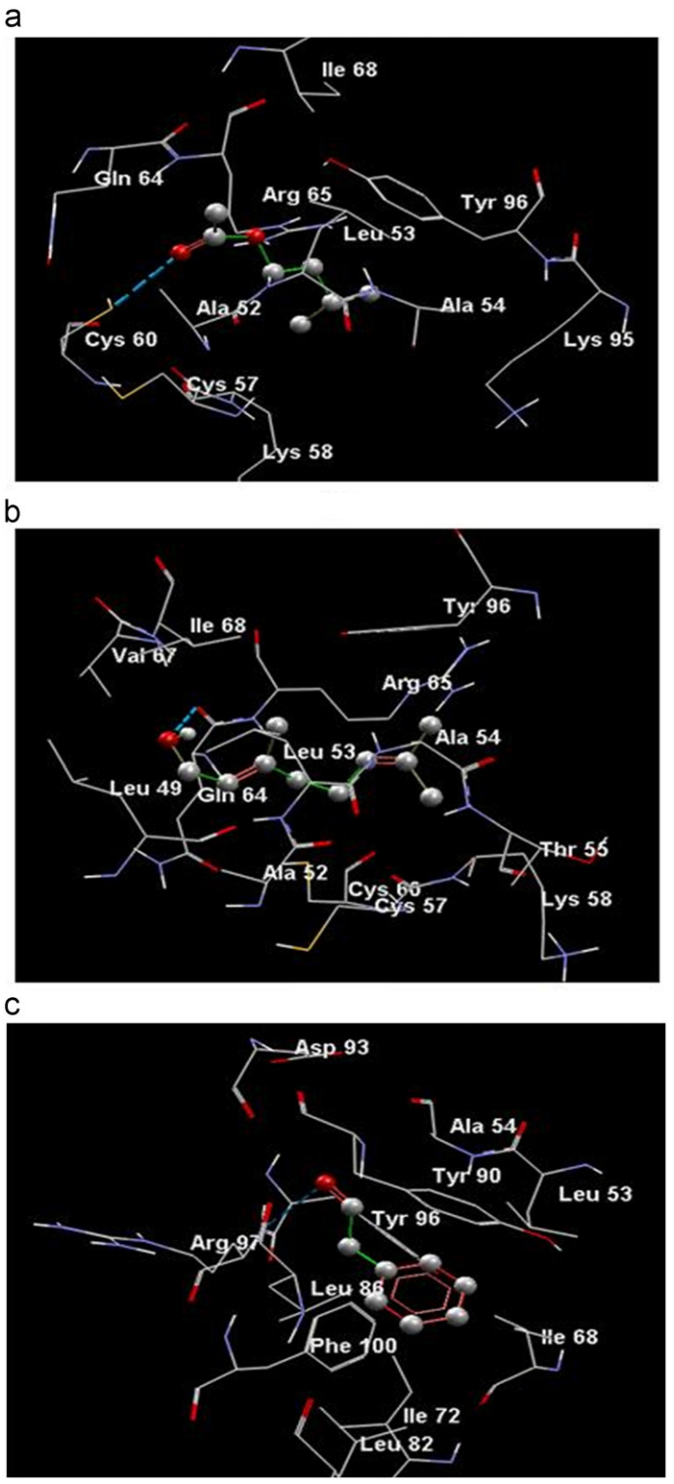

Fig. 5. Binding modes of different ligands to Ac-ASP3: (a) isoamyl acetate; (b) geraniol; (c) phenyl acetaldehyde. Only the corresponding parts of the complex of Ac-ASP3 and ligands are shown. Hydrogen bonds are shown with the blue dashed lines. (For interpretation of the references to color in this figure legend, the reader is referred to the web version of this article.)

essence of biological reactions. Therefore, they are helpful for exploring the configuration and physiological function of Ac-ASP3. Based on known conformation of protein and ligands, we can dope out their binding modes with molecular docking. Hence, molecular docking can be used for eliminating improper ligands before starting the experiments, in order to save manpower and material resources markedly. It is able to improve the convenience and rapidity of correlative study.

The ligand binding can induce the conformational changes of Ac-ASP3 (Pelosi et al., 2005). From the simulation of the ligand-protein binding reactions, we could get that the reactions have changed the backbone and rotated the side chains of the protein molecule. Some theoretical models have been established for correlations between protein electrical properties and their conformation (Alfinito et al., 2008; Alfinito et al., 2010). In these models, each amino acid is taken as a node and replaced with a sphere, whose position coincides with its C_α atom, shown in Fig. 6a. Each couple of nodes is connected with a link, when their distance $l_{i,j}$ is less than an assigned interacting radius R_c. The optimal value of R_c should be in the range of 5–15 Å. We can acquire the impedance network when an elementary impedance is attributed to each link, shown in Fig. 6b. Corresponding to the simplified Randles cell, Rct-CPE parallel circuit, a RC parallel circuit could be chosen as the elementary impedance. This perspective is able to reconcile the view of the charge (specifically electron) transport inside the protein. Then, the impedance spectrum of protein depending on the distance between nodes at certain frequency range can be expressed in the form of a Nyquist plot.

Through the ligand binding, the backbone displacement mainly contributes to the changes of the electrical properties. When the protein changes from its native state to activated state, the α-helices of the protein change their relative distance, inducing change of the value of $l_{i,j}$ in the network, then leading to the variety of $Z_{i,j}$, which determines the shift of the global impedance spectrums of the biosensor. With the complementarities of the structure of Ac-ASP3 both in native state and activated state, the correlation between the change of protein conformation and change of protein electrical properties should be obtained definitely.

Molecular modeling has been promoting quantificational and modeling progress in life sciences. Combing with experiments, it is conducive to studies on biological phenomena and helps to provide the basis for information processing methods together with system development. By the combination of the molecular modeling with impedance detection, CSPs will provide a promising approach for chemical molecular sensing with their natural chemosensory abilities.

4. Conclusions

We have developed an impedance olfactory biosensor using CSPs from honeybee. The availability of large amount of recombinant CSPs has overcome the difficulty to obtain biology sensing material. By recording the impedance spectroscopy, specific pheromones and floral odors, such as isoamyl acetate, geraniol and phenyl acetaldehyde produced detectable and linear impedance variation with increasing concentration, with a detection limit of micromole. With the aid of molecular modeling, we identified the conserved amino acids within the binding site and established the correlations between protein-ligand binding characteristics and impedance spectra change. With molecular modeling, we can improve accuracy, specificity and predictability of the ligands binding to the protein and optimize the design of the sensor. Chemosensation is used in locating food and avoiding predators, pathogens and toxins, etc. by honeybee. The design of the CSP based biosensor provides a platform, which could apply olfactory systems to detecting pheromones and floral odors selectively and quantitatively. Further more, it could be used in beekeeping, environmental monitoring, anti-bioterrorism, disease diagnostics and food safety.

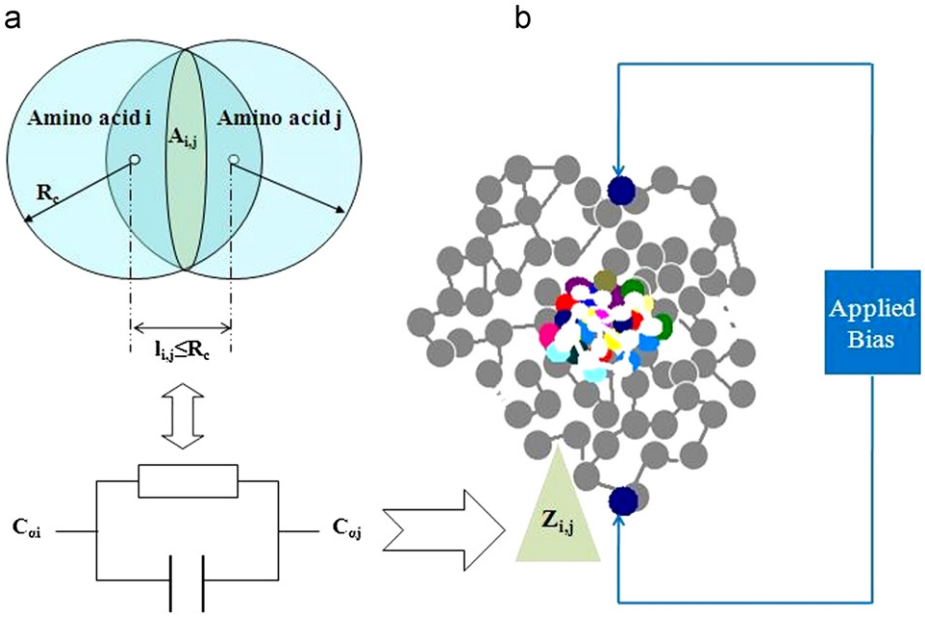

Fig. 6. (a) The link between amino acids and its equivalent impedance elementary RC circuit. (b) Cartoon of the protein mapped into an impedance network: the colorful balls indicate ligand molecule. (For interpretation of the references to color in this figure legend, the reader is referred to the web version of this article.)

Acknowledgments

This work was supported by the National Natural Science Foundation of China (Grant No. 81071226, 60725102, 21107094, 30900163), the Research on Public Welfare Technology Application Projects of Zhejiang Province, China (No. 2011C23096), and the Fundamental Research Funds for the Central Universities.

Appendix A. Supporting information

Supplementary data associated with this article can be found in the online version at http://dx.doi.org/10.1016/j.bios.2012.07.011.

References

Abassi, Y.A., Jackson, J.A., Zhu, J., O'Connell, J., Wang, X., Xu, X., 2004. Journal of Immunological Methods 292, 195–205.
Alfinito, E., Millithaler, J.-F., Pennetta, C., Reggiani, L., 2010. Microelectronics Journal 41, 718–722.
Alfinito, E., Pennetta, C., Reggiani, L., 2008. Nanotechnology 19 (065202), 1–12.
Atienza, J.M., Yu, N., Kirstein, S.L., Xi, B., Wang, X., Xu, X., Abassi, Y.A., 2006. ASSAY and Drug Development Technologies 4 (5), 597–607.
Briand, L., Swasdipan, N., Nespoulous, C., Bézirard, V., Blon, F., Huet, J.C., Ebert, P., Pernollet, J.C., 2002. European Journal of Biochemistry 269, 4586–4596.
Buck, L., Axel, R., 1991. Cell 65, 175–187.
Forêt, S., Wanner, K.W., Maleszka, R., 2007. Insect Biochemistry and Molecular Biology 37, 19–28.
Glatz, R., Bailey-Hill, K., 2011. Progress in Neurobiology 93, 270–296.
Hou, Y., Jaffrezic-Renault, N., Martelet, C., Tlili, C., Zhang, A., Pernollet, J., Briand, L., Gomila, G., Errachid, A., Samitier, J., Salvagnac, L., Torbiéro, B., Temple-Boyer, P., 2005. Langmuir 21, 4058–4065.
Katz, E., Willner, I., 2003. Electroanalysis 15 (11), 913–947.
Ko, H.J., Park, T.H., 2008. Biosensors & Bioelectronics 23, 1017–1023.
Kubinyi H. 2001. In Pharmacokinetic optimization in drug research: biological, physicochemical, and computational strategies, 1st ed; Testa, B.; van de Waterbeemd, H.; Folkers, G.; Guy, R. Helvetica Chimica Acta: Zürich, Switzerland, 513–524.
Lee, S.H., Park, T.H., 2010. Biotechnology and Bioprocess Engineering 15, 22–29.
Li, H., Lou, B., Cheng, J., Gao, Q., 2007. Chinese Science Bulletin 52, 1355–1364.
Lisdat, F., Schäfer, D., 2008. Analytical and Bioanalytical Chemistry 391, 1555–1567.
Liu, Q., Ye, W., Xiao, L., Du, L., Hu, N., Wang, P., 2010. Biosensors & Bioelectronics 25, 2212–2217.
Minic, J., Grosclaude, J., Aioun, J., Persuy, M.A., Gorojankina, T., Salesse, R., Pajot-Augy, E., Hou, Y., Helali, S., Jaffrezic-Renault, N., Bessueille, F., Errachid, A., Gomila, G., Ruiz, O., Samitier, J., 2005. Biochimica et Biophysica Acta 1724, 324–332.
Nocker, M, Handschuh, S, Tautermann, C, Liedl, KR., 2009. Journal of Chemical Information and Modeling 49 (9), 2067–2076.
Ozaki, K., Utoguchi, A., Yamada, A., Yoshikawa, H., 2008. Insect Biochemistry and Molecular Biology 38, 969–976.
Pelosi, P., Calvello, M., Ban, L., 2005. Chemical Senses 30, i291–i292.
Picimbon, J.F., Dietrich, K., Breer, H., Krieger, J., 2000. Insect Biochemistry and Molecular Biology 30, 233–241.
Picone, D., Crescenzi, O., Angeli, S., Marchese, S., Brandazza, A, Ferrara, L., Pelosi, P., 2001. European Journal of Biochemistry 268, 4794–4801.
Rains, G.C., Tomberlin, J.K., 2008. Kulasiri D 26, 288–294.
Repasky, K.S., Shaw, J.A., Scheppele, R, Melton, C., Carsten, J.L., Spangler, L.H., 2006. Applied Optics 45, 1839–1843.
Sankaran, S., Panigrahi, S., Mallik, S., 2010. Biosensors and Bioelectronics 26, 3103–3109.
Vidic, J., 2010. Intelligent and Biosensors, 377–386.
Vieira, F.G., Rozas, J., 2011. Biology and Evolution 3, 476–490.
Zhang, Y., 2008. BMC Bioinformatics 9, 40.